

## Electronic Supplemental Information:

### 1. Experimental Section

#### 1.1 Synthesis of n-type ZnFe<sub>2</sub>O<sub>4</sub> and p-type Co-ZnFe<sub>2</sub>O<sub>4</sub>

The n-type ZnFe<sub>2</sub>O<sub>4</sub> film was prepared by the hydrothermal method. The FTO was ultrasonically cleaned through acetone, isopropanol, ethyl alcohol absolute and deionized water, respectively. The cleaned FTO was kept in a Teflon lined stainless steel autoclave. 0.15 M FeCl<sub>3</sub>·6H<sub>2</sub>O, 0.10 M Zn(NO<sub>3</sub>)<sub>2</sub>·6H<sub>2</sub>O and 0.15 M NaNO<sub>3</sub> were dissolved in 20 mL deionized water, stirring for 15 min to obtain precursor solution, which was poured into the Teflon lined stainless steel autoclave for 6 h at 100 °C. Then, the FTO was cleaned in deionized water and dried in air. Subsequently, the FTO was sintered at 550 °C for 2 h. After sintering, the FTO was immersed in 1 M NaOH solution for 12 h to remove unwanted ZnO thin layer. Eventually, the n-type ZnFe<sub>2</sub>O<sub>4</sub> film was prepared. Most of the preparation progress of p-type Co-ZnFe<sub>2</sub>O<sub>4</sub> was similar to that of n-type ZnFe<sub>2</sub>O<sub>4</sub>. The only difference was that 0.04 M Co(NO<sub>3</sub>)<sub>2</sub>·6H<sub>2</sub>O was added to the precursor solution. Other conditions were remained unchanged.

#### 1.2 Characterizations

The morphology and microstructure of samples were carried out on JEOL JSM-7800F scanning electron microscope (SEM) and JEOL JEM-2100 transmission electron microscopy (TEM). The crystal structures of samples were determined from data using an X-ray diffractometer (XRD, Rigaku-D/max-2500; Cu K $\alpha$  radiation,  $\lambda=0.154059$  nm, 40 kV, 150 mA). The elements of samples were identified via energy dispersive X-ray spectroscopy (EDS, AZtec from Oxford). The surface chemical states of samples were recorded by X-ray photoelectron spectroscopy (XPS, Thermo ESCALAB 250Xi). The Fourier transform infrared (FTIR) spectrometry of samples were measured by RXI FTIR Spectrometer. The optical absorption performance of samples was examined by DU-8B UV-vis double-beam spectrophotometer. The PEC performance was probed in 0.5 M Na<sub>2</sub>SO<sub>4</sub> electrolyte without sacrificial agent (pH=7), a standard three-electrode configuration that prepared films as working electrode, a platinum foil as counter electrode and an Ag/AgCl (in saturated KCl) electrode as reference electrode via an electrochemical workstation and irradiated with a Xenon lamp (AM 1.5 G, 100 mW·cm<sup>-2</sup>). The electrochemical impedance spectra (EIS) was collected on a three-electrode configuration, recorded under illumination at a potential of 0 V vs RHE and a frequency range of 10-100 kHz. The gas amounts of H<sub>2</sub> and O<sub>2</sub>

were measured by a gas chromatograph.

The average grain size of samples was calculated by the Debye-Scherrer formula as follows [S1]:

$$D=0.94\lambda/\beta\cos\theta \quad (1)$$

Where D was the grain size,  $\lambda$  was the wavelength of radiation ( $\lambda=0.154059$  nm),  $\theta$  was the Bragg diffraction angle,  $\beta$  was the full width at half maximum on a  $2\theta$  scale.

The optical band gap was calculated as follows [S2]:

$$(\alpha h\nu)^n=A(h\nu-E_g) \quad (2)$$

Where  $\alpha$  was the absorption coefficient,  $h$  was the Planck's constant,  $\nu$  was the photon frequency, the  $n$  was 2 or 1/2 according to a direct or indirect band gap semiconductor,  $A$  was a constant and  $E_g$  was the optical band gap.

The Mott-Schottky plot was carried out in 0.5 M  $\text{Na}_2\text{SO}_4$  solution to estimate the flat band potential of samples, the calculation was according to the following equations [S3, S4]:

$$\text{n-type semiconductor: } 1/C^2=(2/e_0\epsilon\epsilon_0N_d)[(V_a-V_{fd})-kT/e_0] \quad (3)$$

$$\text{p-type semiconductor: } 1/C^2=(2/e_0\epsilon\epsilon_0N_A)[(-V_a+V_{fd})-kT/e_0] \quad (4)$$

Where  $C$  was the specific capacitance,  $e_0$  was fundamental electric charge,  $\epsilon$  was the dielectric constant,  $\epsilon_0$  was the permittivity of vacuum,  $N_d$  was the donor density (n-type semiconductor),  $N_A$  was the acceptor density (p-type semiconductor),  $V_a$  was the applied potential,  $V_{fd}$  was the flat band potential,  $k$  was the Boltzmann constant and  $T$  was the temperature.

The collected Ag/AgCl potential was converted to the reversible hydrogen electrode (RHE) potential as follows [S5]:

$$E_{\text{RHE}}=E_{\text{Ag/AgCl}}+0.059\text{pH}+0.1976 \text{ V} \quad (5)$$

### **Lists of the Figures:**

Fig.S1 Survey XPS spectrum of Co-ZnFe<sub>2</sub>O<sub>4</sub>

Fig.S2 Cell structure of spinel structure ZnFe<sub>2</sub>O<sub>4</sub>

Fig.S3 FTIR spectra of samples: (a) wavenumbers from 4000 cm<sup>-1</sup> to 350 cm<sup>-1</sup>, (b) magnified view from 1500 cm<sup>-1</sup> to 450 cm<sup>-1</sup>

Fig.S4 Optical indirect band gap energy ( $E_g$ ) of samples

Fig.S5 XPS valence band spectrum (a) and enlarged spectrum (b) of ZnFe<sub>2</sub>O<sub>4</sub>, XPS valence band spectrum (c) and enlarged spectrum (d) of Co-ZnFe<sub>2</sub>O<sub>4</sub>

Fig.S6 Chopped J-V curves (a), equivalent circuit model and related parameters of electrochemical impedance spectra (b) of ZnFe<sub>2</sub>O<sub>4</sub> and Co-ZnFe<sub>2</sub>O<sub>4</sub>

Fig.S7 J-V curves (a), chopped J-V curves (b), electrochemical impedance spectra (c), equivalent circuit model and related parameters of electrochemical impedance spectra (d) of different concentrations of cobalt doped ZnFe<sub>2</sub>O<sub>4</sub>

Fig.S8 Diagrammatic sketch about the charge transfer of the dual photoelectrodes stacked system

Fig.S9 J-V curves of n-type ZnFe<sub>2</sub>O<sub>4</sub> and p-type Co-ZnFe<sub>2</sub>O<sub>4</sub> (a), J-t curve with no applied bias (b) and gas production (c) of the dual photoelectrodes stacked system

Fig.S10 Diagrammatic sketch about the charge transfer of Co-ZnFe<sub>2</sub>O<sub>4</sub> nanorods

Tab.S1 Summary of XPS data about Zn 2p, Fe 2p, O 1s, Co 2p and C 1s of Co-ZnFe<sub>2</sub>O<sub>4</sub>

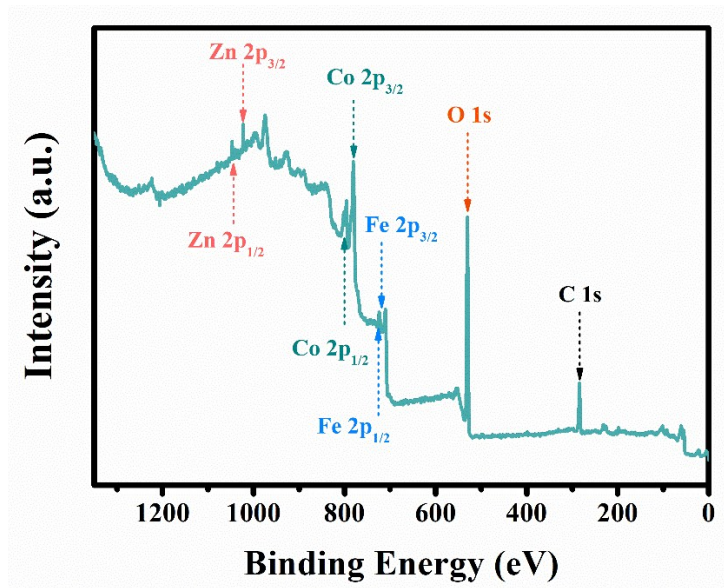


Fig.S1 Survey XPS spectrum of Co-ZnFe<sub>2</sub>O<sub>4</sub>

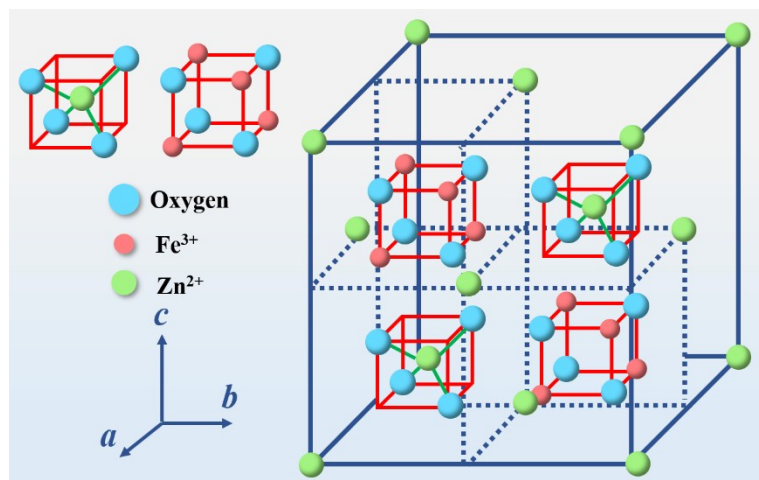


Fig.S2 Cell structure of spinel structure ZnFe<sub>2</sub>O<sub>4</sub>

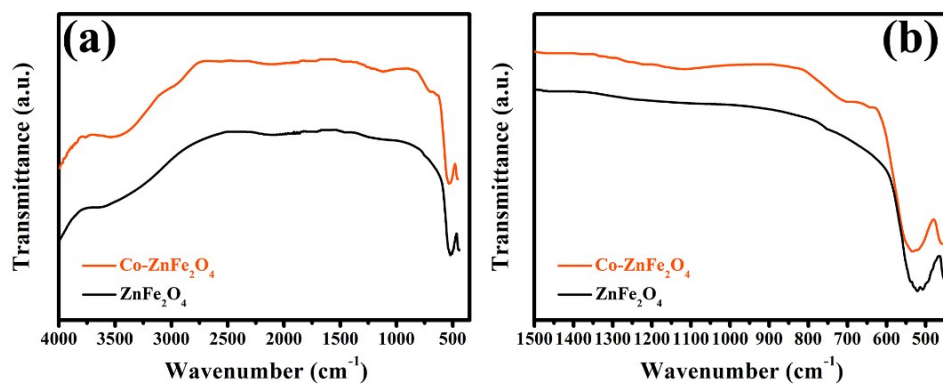


Fig.S3 FTIR spectra of samples: (a) wavenumbers from 4000 cm<sup>-1</sup> to 350 cm<sup>-1</sup>, (b) magnified view from 1500 cm<sup>-1</sup> to 450 cm<sup>-1</sup>

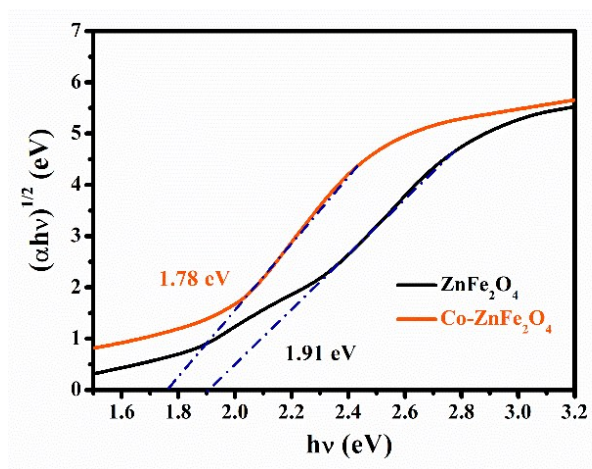


Fig.S4 Optical indirect band gap energy ( $E_g$ ) of samples

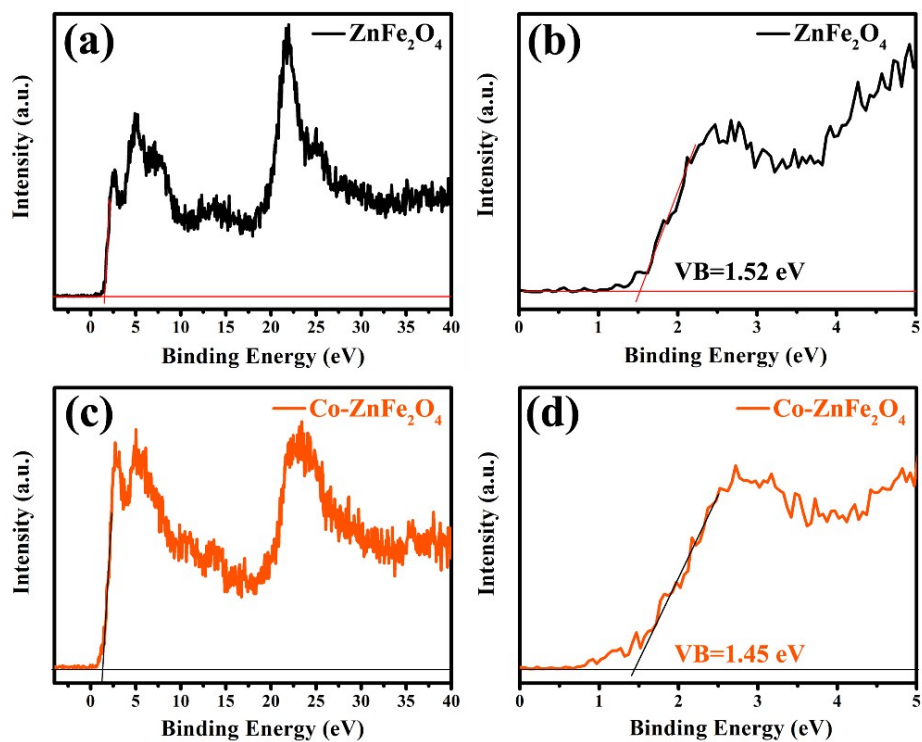


Fig.S5 XPS valence band spectrum (a) and enlarged spectrum (b) of  $\text{ZnFe}_2\text{O}_4$ , XPS valence band spectrum (c) and enlarged spectrum (d) of  $\text{Co-ZnFe}_2\text{O}_4$

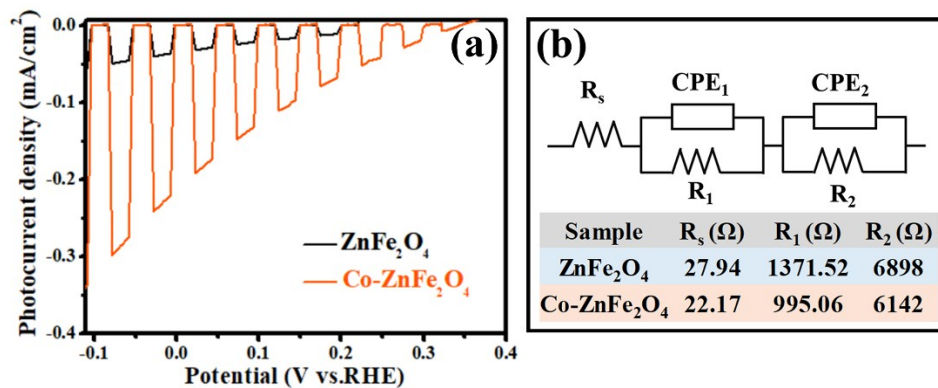


Fig.S6 Chopped J-V curves (a), equivalent circuit model and related parameters of electrochemical impedance spectra (b) of  $\text{ZnFe}_2\text{O}_4$  and  $\text{Co-ZnFe}_2\text{O}_4$

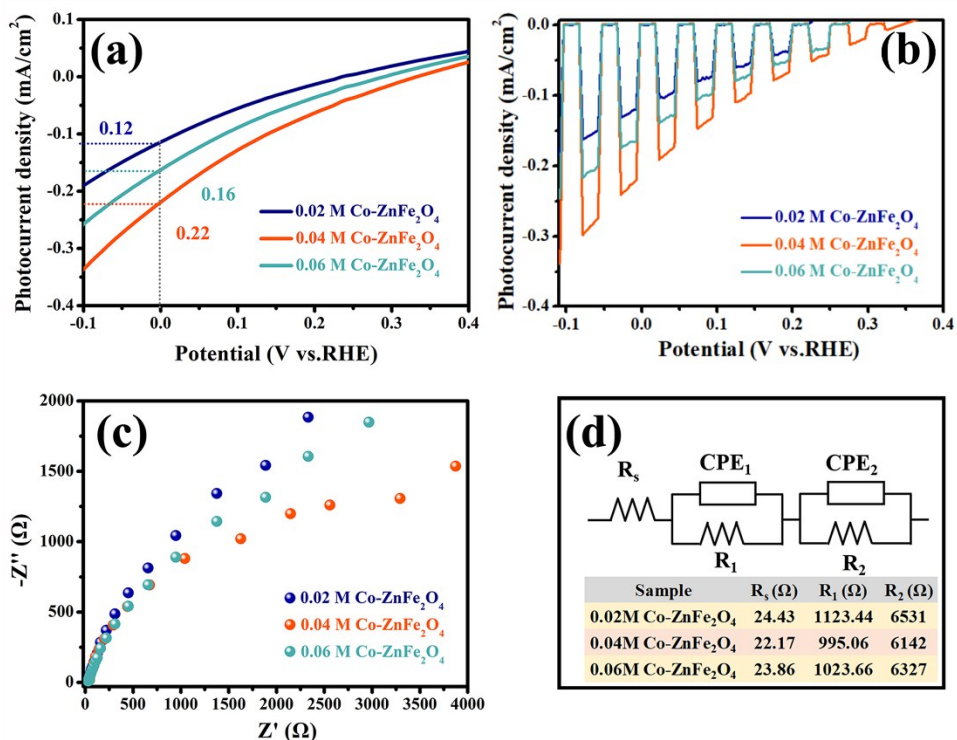


Fig.S7 J-V curves (a), chopped J-V curves (b), electrochemical impedance spectra (c), equivalent circuit model and related parameters of electrochemical impedance spectra (d) of different concentrations of cobalt doped ZnFe<sub>2</sub>O<sub>4</sub>

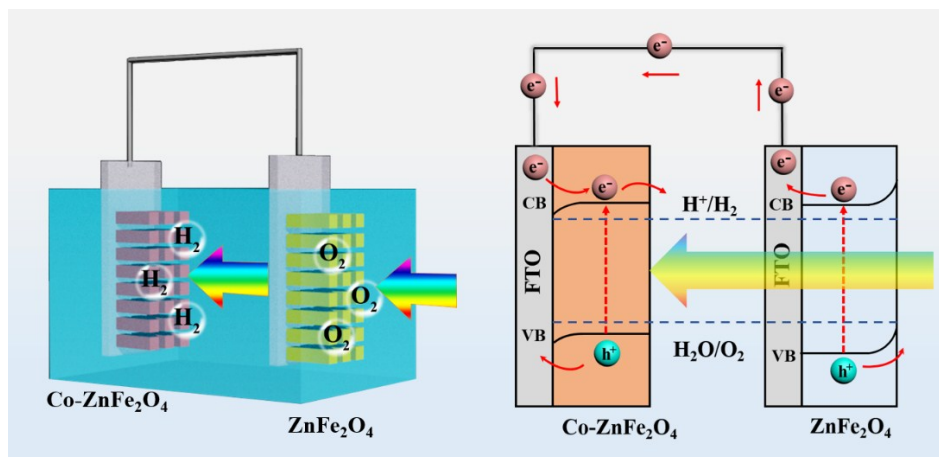


Fig.S8 Diagrammatic sketch about the charge transfer of the dual photoelectrodes stacked system

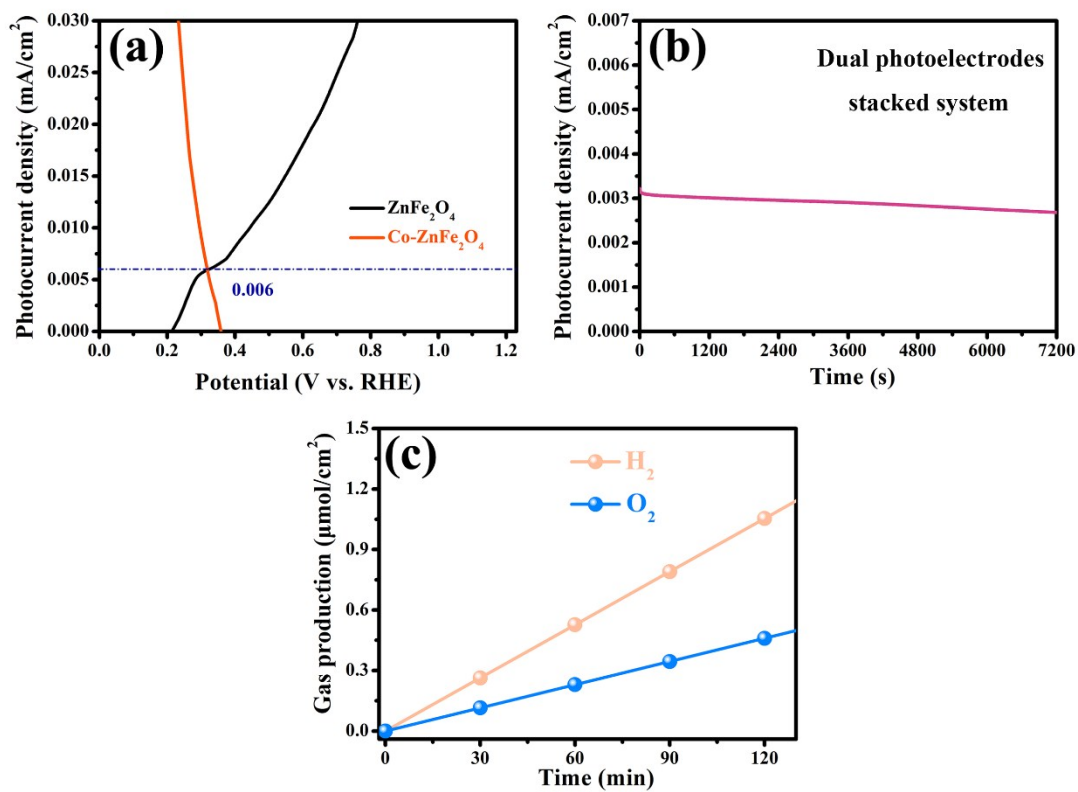


Fig.S9 J-V curves of n-type  $\text{ZnFe}_2\text{O}_4$  and p-type  $\text{Co-ZnFe}_2\text{O}_4$  (a), J-t curve with no applied bias (b) and gas production (c) of the dual photoelectrodes stacked system

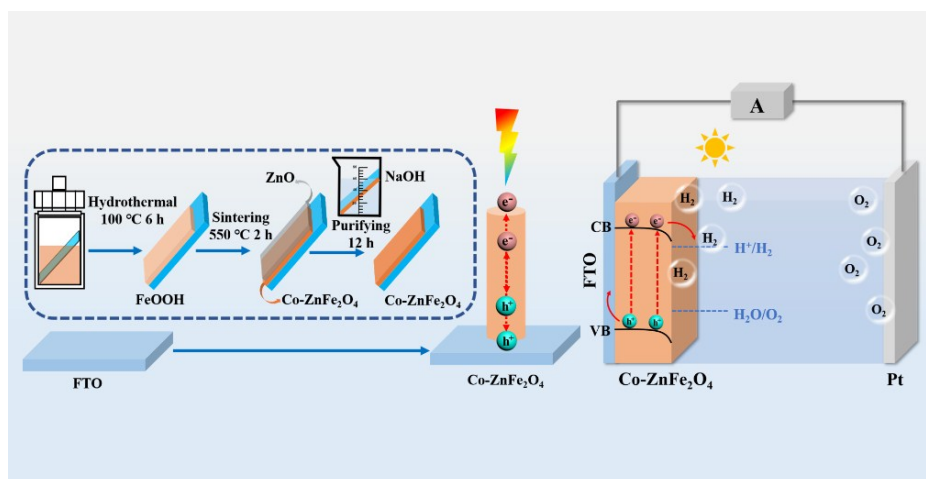


Fig.S10 Diagrammatic sketch about the charge transfer of  $\text{Co-ZnFe}_2\text{O}_4$  nanorods

Tab.S1 Summary of XPS data about Zn 2p, Fe 2p, O 1s, Co 2p and C 1s of Co-ZnFe<sub>2</sub>O<sub>4</sub>

Name	Atomic %	Start BE	End BE	Peak BE	Height CPS	Area (P) CPS.eV	Peak Type
Zn 2p	11.59	1058.67	1014.71	1022.81	12710.323	11996.41	Standard
Fe 2p	23.18	745.04	698.31	710.78	64893.762	67681.44	Standard
O 1s	46.37	539.15	524.44	529.73	134010.793	258564.19	Standard
Co 2p	2.24	815.69	768.82	780.93	28788.643	510661.82	Standard
C 1s	16.62	296.55	281.55	284.74	20864.942	29390.57	Standard

### References:

- [S1] Z. Zhang, M. F. Hossain and T. Takahashi, *Int. J. Hydrogen Energy*, 2010, 35, 8528-8535.
- [S2] M. Chandrika, A. V. Ravindra, C. Rajesh, S. D. Ramarao and S. Ju, *Mater Chem Phys*, 2019, 230, 107-113.
- [S3] W. Ma, X. Wu, K. Huang, M. Wang, R. Fu, H. Chen and S. Feng, *Sus. Energy. Fuels*, 2019, 3, 2135-2141.
- [S4] Y. Xu, J. Jian, F. Li, W. Liu, L. Jia and H. Wang, *J. Mater. Chem. A*, 2019, 7, 21997-22004.
- [S5] M. Li, L. Chen, C. Zhou, C. Jin, Y. Su and Y. Zhang, *Nanoscale*, 2019, 11, 18071-18080.